



## Strategy for creating rational fraction fits to stabilization graph data on metastable electronic states

K. Gasperich<sup>a</sup>, K.D. Jordan<sup>a,\*</sup>, J. Simons<sup>b</sup>

<sup>a</sup> Department of Chemistry, University of Pittsburgh, Pittsburgh, PA 15260, United States

<sup>b</sup> Department of Chemistry, University of Utah, Salt Lake City, UT 84112, United States

### ABSTRACT

An exactly soluble model of two diabatic electronic states interacting through a coupling of strength  $V$  is used to generate data for testing the rational fraction analytic continuation technique for determining the energies and widths of metastable states of anions. By making analytical connections between the coefficients in the rational fraction and the parameters of the model, we are able to suggest how to choose the orders of the polynomials and the range of the scaling parameter,  $Z$ , within which to compute the energies for a given precision. This analysis also allows us to specify the range of  $Z$ -values to use in constructing the rational fraction in a manner that allows determination of all parameters of the model for a given precision. The constraint on the  $Z$ -value ranges can be used as a guide for constructing rational fractions of data obtained in electronic structure calculations on actual resonance states.

### 1. Introduction

When treating metastable electronic states of atomic and molecular anions, the stabilization technique introduced by Hazi and Taylor [1] has proven to be very useful. In its most commonly employed form, the energies of several electronic states of the excess-electron system are computed for a range of values of a parameter ( $Z$ ) that controls the radial extent of the basis functions used in the calculations [2]. These energies are then plotted as functions of the parameter  $Z$  to generate stabilization plots such as that shown in Fig. 1.

Such stabilization plots typically display three characteristics that merit attention:

1. One or more plateau regions within which the energy of one of the branches changes slowly as the scaling parameter is varied. In Fig. 1, such plateaus occur at energies near 0.45 and 1.35 eV. The energies of the plateau regions approximate the energies of the metastable electronic states being studied.
2. A series of states whose energies change more rapidly as the scaling parameter is varied; these energies describe pseudo-continuum states that correspond to the neutral molecule plus a “free” electron in a pseudo-continuum orbital. In Fig. 1 the energies of these states increase with the scaling parameter  $Z$  which controls the radial extent of the basis set.
3. As  $Z$  is varied, one encounters regions where two types of states approach one another and undergo avoided crossings. The regions of these avoided crossings play a central role in determining the

lifetime of the metastable state. In Fig. 1 we see that the plateau regions are interrupted by a series of avoided crossings thus limiting the range of  $Z$ -values over which any given plateau persists.

There is another class of stabilization methods that involves adding a stabilizing potential that converts the resonance into a bound state followed by analytically continuing the bound-state energy into the resonance region [3]; however, we do not consider these approaches here.

The example illustrated in Fig. 1 shows how the energies of several excess-electron states vary as the scaling parameter is changed. Electronic structure methods such as configuration interaction, equations-of-motion coupled cluster (EOM-CC) [4,5], Koopmans’ theorem [6], and many-body Green’s functions [7] can be used to extract multiple roots as functions of the scaling parameter, it is then usually relatively straightforward to identify regions of avoided-crossings within a range of  $Z$ -values. The rational fraction (RF) method, which is the subject of this study, is designed to fit the energy of a single root of the stabilization calculation as a function of the scaling factor, and it is usually a root whose energy lies within a plateau region that is used [8].

### 2. Extracting the energy and lifetime of the metastable state from a stabilization plot

#### 2.1. RF and quadratic equation approaches for fitting stabilization-plot data

In the Siegert picture [9], a metastable state, also called a

\* Corresponding author.

E-mail address: [jordan@pitt.edu](mailto:jordan@pitt.edu) (K.D. Jordan).

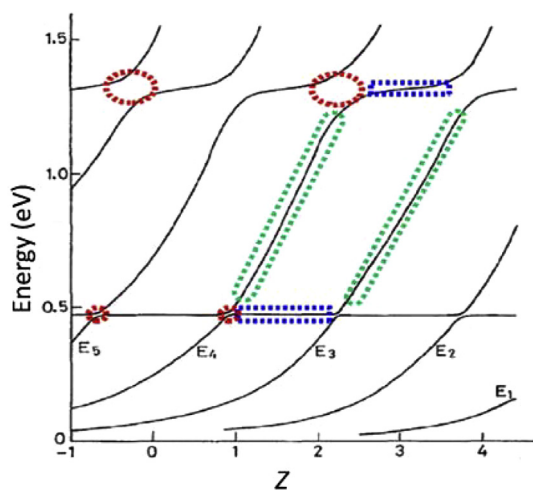


**Fig. 1.** Example of a stabilization plot of the energies of several excess-electron states relative to the energy of the corresponding neutral for the case where increasing the parameter  $Z$  scales the radial extent of the basis set. The curves in black are reproduced from A. Macias and A. Riera, *The Journal of Chemical Physics*, 96, 2877 (1992)], with the permission of AIP Publishing. The colored dashed regions were added by the present authors. The regions surrounded in blue illustrate two of the plateaus, those in red illustrate four of the avoided crossings, and those in green illustrate two of the pseudo-continuum regions (see text).

resonance, is associated with a complex energy  $E_R - i\Gamma/2$ , where  $E_R$  is the resonance position and  $\Gamma$  the width is proportional to the reciprocal of the lifetime. This complex energy, when substituted into  $e^{-iEt/\hbar}$ , describes a state that decays in time. Correspondingly, one can view such a state as having an energy uncertainty (or width)  $\Gamma$ . The resonance parameters  $E_R$  and  $\Gamma$  can be obtained by analytically continuing the energy as a function of  $Z$  into the complex plane, locating the stationary points  $Z_{sp}$  where  $\partial E/\partial Z = 0$ , and then evaluating  $E$  at  $Z_{sp}$  [10]. In the RF method, analytic continuation is performed after using computed energy values to construct a rational fraction:

$$E(Z) = \frac{N(Z)}{D(Z)} \quad (1)$$

where

$$N(Z) = \sum_{j=0}^{j=n} n_j Z^j \quad (2)$$

and

$$D(Z) = \sum_{j=0}^{j=d} d_j Z^j \quad (3)$$

When the coefficients in the numerator and denominator are determined from the coefficients of a Taylor series expansion of a function, the RF is also referred to as a Padé approximant [11]; when the coefficients are determined using numerical data giving  $E$  at various  $Z$ -values, the term RF is preferred.

The  $[n, d]$  approximant has  $n + d + 2$  parameters; however, only  $n + d + 1$  of these are independent, because the energy depends on the ratio  $N/D$  rather than on  $N$  and  $D$  individually. Often, one opts to set  $d_0 = 1$ , but other choices are possible. After using the computed energies to determine the values  $\{n_j, d_j\}$  of the expansion coefficients, the derivative of the energy with respect to  $Z$  is evaluated and set equal to zero,

$$\frac{\partial E}{\partial Z} = 0 \quad (4)$$

Solving Eq. (4) for the  $Z$ -values at which this equation holds gives

the complex stationary points  $Z_{sp}$ , which are then substituted into the rational fraction expression to generate complex stationary energies

$$E_{sp} = E_R \pm i\Gamma/2 \quad (5)$$

Although the primary goal of this paper is to analyze the RF method, it is useful to also consider the alternative quadratic equation (QE) approach [2,10,12], in which one introduces the following expression for how the energy  $E$  varies with the scaling parameter  $Z$ :

$$P(Z)(E(Z))^2 + Q(Z)E(Z) + R(Z) = 0 \quad (6)$$

where  $P$ ,  $Q$ , and  $R$  are polynomials in  $Z$ :

$$P(Z) = \sum_{j=0}^{j=p} p_j Z^j \quad (7)$$

$$Q(Z) = \sum_{j=0}^{j=q} q_j Z^j \quad (8)$$

$$R(Z) = \sum_{j=0}^{j=r} r_j Z^j \quad (9)$$

This expression has  $p + q + r + 3$  total parameters, but, as with the RF, the energy is unchanged when all polynomials in  $Z$  are scaled by a constant factor; therefore, the number of independent parameters is  $p + q + r + 2$ , and a common choice is to set  $p_0$  equal to unity. After the polynomial coefficients  $\{p_j, q_j, r_j\}$  are determined by fitting, one solves for  $E$ , obtaining

$$E(Z) = -\left[\frac{Q(Z)}{2P(Z)}\right] \pm \sqrt{\left[\frac{Q(Z)}{2P(Z)}\right]^2 - \frac{R(Z)}{P(Z)}} \quad (10)$$

The derivative of the energy expression in Eq. (10) with respect to  $Z$  is then set to zero to determine (complex) values of  $Z$  at which  $E(Z)$  is stationary, which are then substituted into Eq. (10) to generate the complex energies associated with the stationary points, yielding  $E_{sp} = E_R \pm i\Gamma/2$  as discussed above. In general, the stationary points  $Z_{sp}$  associated with a resonance arising from a pair of coupled diabatic states are not far from the complex branch points associated with the avoided crossing between discrete and pseudo-continuum diabatic states [10]. The branch points of Eq. (10) occur at values of  $Z$  where  $Q^2(Z) - 4P(Z)R(Z) = 0$ . The QE framework builds into its working equations the existence of branch points, whereas the RF method does not.

If one utilizes the same number of  $E(Z_k)$  data points as one has parameters in either the RF or QE analytic continuation expression, one obtains a system of linear equations to be solved for the polynomial coefficients. In the RF approach, one can cast the problem in the form of a continued fraction, which allows the coefficients to be determined by a recursion relation [13]. Alternatively, one can employ more data points than parameters and use a least-squares procedure to optimize the parameters. The details of how one fits the calculated energy values to either Eq. (1) or Eq. (6) will not be further discussed in this work; rather our focus will be on how to determine optimal ranges of  $Z_k$  values used to compute the energies used in the fits and what order of polynomials should be used in the RF fits.

## 2.2. Selecting data points for RF fits that are not too far from avoided crossings

Pairs of diabatic states of the same symmetry that cross as the scale parameter is varied undergo avoided crossings when they are allowed to interact as shown in Fig. 1, resulting in adiabatic energies that display complex branch points. This behavior is the primary motivation for introducing the QE analytic continuation procedure. In the QE approach, the data for the fitting generally employs data points from the vicinity of an avoided crossing but may also include values more distant

from the avoided crossing; moreover, in the QE approach, the data points can be chosen from a single branch or from both branches involved in the chosen avoided crossing. RFs of the form given in Eq. (1) do not properly describe the branch points but generally have poles and zeros at  $Z$ -values close to where the diabatic states cross. If one were performing the analytic continuation using a simple power series, one would then have to avoid data points “close” to the crossing point of the diabatic curves because such points might be outside the radius of convergence of the series. With RFs, this is less of an issue as convergence can be achieved even when using data points close to the crossing region, although the inclusion of such points may slow down the rate of convergence, and, in practice, one often avoids using such data points.

As we illustrate later, the RF approach will not be able to accurately describe the resonance if one only uses data points from a stabilization plot that are “far” from the avoided crossing. In that case, the  $E(Z)$  vs.  $Z$  data contain too little information about the strength of the coupling between the two diabatic states. A main goal of this work is to provide a path by which one can estimate how close to the crossing point one must include  $E(Z)$  data points given the precision to which one knows the  $Z$ -variation of the energies contained in the stabilization plot. Alternatively, we show to what precision one must, if feasible, determine the  $E$ -values for a given choice of  $Z$ -values.

### 3. Model for which the exact energy and width are known

#### 3.1. What is the purpose of introducing an analytically solvable model?

We use  $E(Z)$  vs.  $Z$  data generated from a model's exact solution and from expansions of the model's exact solution valid through various orders in the coupling strength  $V$  to illustrate the problems that arise if one employs data points too far from a crossing point in forming a RF. We provide explicit formulas, in terms of the model's parameters, for the ranges of  $Z$  within which data should be calculated given the precision  $\varepsilon$  to which variations in the energies  $E(Z)$  are known as  $Z$  varies and given the order in  $V$  to which one wishes to determine the resonance state's width.

We suggest that the lessons learned from testing RF methodology on this exactly soluble model can be applied to ab initio electronic structure stabilization graphs. In particular, by using data from an ab initio stabilization graph's plateau-region and from its region approaching an avoided crossing to make connections to the model's parameters, the analytical expressions obtained for the model can be used to estimate the range of  $Z$ -values to use in creating an RF fit to the ab initio data.

#### 3.2. The model energy expression and its resonance energy and width

The avoided crossings that pairs of diabatic states undergo can be qualitatively described using a two-state Hamiltonian matrix whose diagonal elements  $H_{11}$  and  $H_{22}$  describe the energies of the diabatic states as functions of the scaling parameter and whose off-diagonal element  $V$  describes the coupling. The two eigenvalues of the resulting matrix are given by  $\frac{1}{2}\{(H_{11} + H_{22}) \pm \sqrt{4V^2 + (H_{22} - H_{11})^2}\}$ . Distant from an avoided crossing, the energies of the diabatic states generally vary monotonically with the scaling factor  $Z$ , which suggests that  $H_{11}$  and  $H_{22}$  can be represented as low-order polynomials in  $Z$ .

The most elementary reasonable model [14] of a stabilization plot's avoided crossing region assumes two diabatic states whose energies vary linearly (in the region of their crossing) with the scaling parameter  $Z$

$$H_{11} = -b_1 + a_1 Z \quad \text{and} \quad H_{22} = -b_2 + a_2 Z \quad (11)$$

These diabatic states intersect at the point

$$Z_0 = \frac{b_2 - b_1}{a_2 - a_1} \quad (12)$$

where their common energy is

$$H_{11}(Z_0) = -b_1 + a_1 Z_0 = H_{22}(Z_0) = -b_2 + a_2 Z_0 = E^0 \quad (13)$$

The parameter  $Z$  could be the factor by which selected diffuse atomic basis functions are scaled. Alternatively, it could be  $(1/R^2)$ , where  $R$  is the radius of a spherical box within which continuum radial basis functions are constrained. In any case, it is best to define  $Z$  in a manner that makes the  $Z$ -dependence of the diabatic pseudo-continuum states as linear as possible.

The energy of the diabatic discrete state (here designated as  $H_{11}$ ) would be expected to be independent of or only weakly dependent on  $Z$ . However, the overlap between the pseudo-continuum basis functions and the discrete state can introduce a  $Z$ -dependence to  $H_{11}$ . Assuming the two orthogonalized diabatic states couple with an off-diagonal Hamiltonian matrix element,  $V$ , solution of the associated  $2 \times 2$  secular equation gives the expression

$$E = E^0 + a(Z - Z_0) \pm \sqrt{V^2 + \left[\frac{\delta a}{2}(Z - Z_0)\right]^2} \quad (14)$$

where  $a = \frac{a_1 + a_2}{2}$  and  $\frac{\delta a}{2} = \frac{a_2 - a_1}{2}$ .

As can be seen from Fig. 1, the diabatic states that undergo an avoided crossing in a stabilization plot do not rigorously vary linearly with the scaling parameter; moreover, although we take  $V$  to be constant within our model, in general it will depend on  $Z$ , because of the  $Z$ -dependence in the coupling between the diabatic states and the impact of the overlap contribution [15]. For these reasons, the analytical results obtained here are certainly approximate representations of stabilization graphs from electronic structure calculations. Our analysis could readily be extended to treat cases in which  $V$  depends on  $Z$  and the diabatic states' energies vary non-linearly with  $Z$ ; however, here we will limit most of our discussion to the simplest case in which the diabatic energies (accounting for overlap between the discrete and pseudo-continuum states) are assumed to vary linearly and  $V$  is assumed to be constant.

In this paper, we use Eq. (14) to generate values of  $E(Z_k)$  to use as input data for Eq. (1) to subsequently determine the energies and widths of the resonance. We do so for three sets of parameters describing resonances with widths differing by a factor of 10 and resonances with clear plateaus and one in which the plateau has a substantial slope. We will refer to energies computed from Eq. (14) as the exact energies for the model problem. We suggest that employing Eq. (14) to generate “test data” to use in Eq. (1) can provide valuable insight into the performance of the RF method for different choices of input data because plots of energies obtained from Eq. (14) display the essential characteristics of actual stabilization plots. Moreover, as we illustrate later, the functional form given in Eq. (14) can offer guidance about what powers of  $Z$  to use and what range of  $Z$ -values to use in forming an effective RF. We suggest that any RF whose polynomials do not contain at least these minimum powers of  $Z$  or that do not use data from the recommended range of  $Z$ -values will not only fail to give accurate resonance energies and widths for the model problem used here but will also fail when applied to stabilization plot data for real chemical systems.

The exact stationary points for the above model are

$$Z_{sp} = Z_0 \pm 2iV \frac{a}{\delta a \sqrt{a_1 a_2}} \quad (15)$$

with the associated energies being

$$E_{sp} = E^0 \pm 2iV \frac{\sqrt{a_1 a_2}}{\delta a} \quad (16)$$

The branch points for the model occur at  $Z_{bp} = Z_0 \pm 2i \frac{V}{\delta a}$ ; hence the stationary points lie further off the real axis than the branch points by a factor of  $a/\sqrt{a_1 a_2}$ .

For the remainder of this paper, we will assume that (i)  $|a_2| > |a_1|$ , (ii) that  $a_2$  and  $a_1$  have the same sign, and (iii) that data from only the

branch having the smaller slope (i.e., the plateau branch with slope  $\alpha_1$ ) is being used to generate the  $E(Z_k)$  data employed in the RF analysis. A similar analysis could be carried out using data from the branch having the larger slope. Moreover, simply for convenience, we will assume that the  $\{Z_k\}$  values are selected to the right of the crossing point  $Z_0$  so that all  $\delta Z_k = Z_k - Z_0$  values are positive.

### 3.3. Guidance offered by the model on how to select powers of $Z$ and $Z'$ values at which to compute energies

The first thing to point out is that Eq. (14) contains five parameters ( $E^0$ ,  $Z_0$ ,  $V$ ,  $a$ , and  $\delta a$ ). Together, the expression for the exact stationary points, Eq. (15) and that for the corresponding resonance energy, Eq. (16) require knowledge of all five of these parameters. This suggests that to accurately predict  $Z_{sp}$  and  $E_{sp}$ , any reasonable RF fit should contain at least five parameters.

As discussed earlier, applications [8] of the RF approach generally utilize  $E(Z_k)$  energies at  $Z_k$  values chosen distant from the avoided crossing region of the stabilization plot to avoid approaching the branch points. As we make more quantitative below, when forming a RF utilizing only  $Z$ -values that are far from the crossing point  $Z_0$  the  $E(Z_k)$  data might not be known with sufficient precision to accurately characterize the stationary point. Although most ab initio electronic structure calculations are performed using double precision arithmetic, issues such as the tolerance to which one converges matrix eigenvalues limit the final precision of the stabilization-plot energy data. Based on our experience, a precision of ca.  $10^{-5}$  eV is a reasonable estimate and one that we use in this paper.

As noted above, RFs with coefficients determined from fitting data points are closely related to PAs where the coefficients are determined by reproducing a fixed number of terms in a power series expansion about an appropriate point. In particular, RFs can be viewed as employing coefficients that correspond to use of derivatives evaluated by numerical differentiation. For that reason, we find it useful to expand Eq. (14) in a power series about a point  $Z'$  chosen to be located approximately in the middle of the set of grid points employed in the RF fit. With the choices of grid points describe above, this necessarily locates  $Z'$  to the right of  $Z_0$  (i.e.,  $Z' > Z_0$ ). The resulting series expansion through terms of order  $(Z - Z')^4$  is:

$$E = E^0 + a\Delta Z \pm K + \left( a \pm \frac{\left(\frac{\delta a}{2}\right)^2 \Delta Z}{K} \right) (Z - Z') \pm \frac{\left(\frac{\delta a}{2}\right)^2 V^2 (Z - Z')^2}{2K^3} \mp \frac{\left(\frac{\delta a}{2}\right)^4 V^2 \Delta Z (Z - Z')^3}{2K^5} \mp \frac{\left(\frac{\delta a}{2}\right)^4 V^2 \Delta Z [5V^2 - 4K^2] (Z - Z')^4}{8K^7} + \dots \quad (17)$$

where  $K = \sqrt{V^2 + \left(\frac{\delta a}{2}\right)^2 \Delta Z^2}$  and  $\Delta Z = Z' - Z_0$ .

For addressing the question concerning the location of  $Z'$ , rather than the distribution of data points around  $Z'$ , we need only substitute  $Z'$  into Eq. (14) giving

$$E = E_0 + a\Delta Z \pm \sqrt{V^2 + \left(\frac{\delta a}{2}\right)^2 \Delta Z^2} \quad (18)$$

If  $Z'$  obeys  $\left| \frac{2V}{\delta a \Delta Z} \right| < 1$ , which it will for points within a plateau region, one can estimate the contributions to  $E$  at various powers of  $V$  by expanding Eq. (18) as

$$E = E^0 + \left( a \pm \frac{\delta a}{2} \right) \Delta Z \pm \frac{V^2}{\delta a \Delta Z} \mp \frac{V^4}{\delta a^3 \Delta Z^3} \pm \dots \quad (19)$$

For the root of Eq. (14) having the smaller (plateau) slope  $\alpha_1$  at large- $Z$  this becomes

$$E = E^0 + \alpha_1 \Delta Z - \frac{V^2}{\delta a \Delta Z} + \frac{V^4}{\delta a^3 \Delta Z^3} + \dots \quad (20)$$

This allows us to specify how close  $Z'$  must be to  $Z_0$  (i.e., how small  $\Delta Z$  must be) for terms proportional to  $V^2$  or  $V^4$  to exceed the precision  $\varepsilon$  to which the electronic structure energies have been computed. In particular, to accurately determine the  $\frac{V^2}{\delta a \Delta Z}$  term in the series expansion requires that  $\Delta Z < \frac{V}{\delta a} \frac{V}{\varepsilon}$ , which is likely achievable in most stabilization calculations as we illustrate later. The next two terms in the energy expansion are  $\frac{V^4}{\delta a^3 \Delta Z^3}$  and  $\frac{2V^6}{\delta a^5 \Delta Z^5}$ . The  $V^4$  and  $V^6$  terms exceed  $\varepsilon$  in magnitude when  $\Delta Z < \frac{V}{\delta a} \left( \frac{V}{\varepsilon} \right)^{\frac{1}{3}}$  and  $\Delta Z < \frac{V}{\delta a} \left( \frac{2V}{\varepsilon} \right)^{\frac{1}{5}}$ , respectively. Later we will show that selecting data in ranges that satisfy  $\Delta Z < \frac{V}{\delta a} \frac{V}{\varepsilon}$  is usually straightforward, but to select data that satisfy the  $V^4$  condition  $\Delta Z < \frac{V}{\delta a} \left( \frac{V}{\varepsilon} \right)^{\frac{1}{3}}$  can be challenging, and to satisfy the  $V^6$  condition is even more so.

### 3.4. Stationary points and energies from the series expansion

The energy expression given by Eq. (17) when truncated at order  $V^2$  has the stationary points

$$Z_{sp} = Z_0 \pm \frac{iV}{\sqrt{\alpha_1 \delta a}} \quad (21)$$

with the corresponding energy

$$E_{sp} = E^0 \pm 2iV \sqrt{\frac{\alpha_1}{\delta a}} \quad (22)$$

Note that even if one knows  $\alpha_1$  from large  $Z$ -results, these expressions for  $E_{sp}$  and  $Z_{sp}$  do not allow one to extract individual values for  $V$  or  $\alpha_2$ .

If we consider the expansion in Eq. (17) through order  $V^4$ , we find

$$Z_{sp} = Z_0 \pm \frac{iVJ}{\sqrt{\alpha_1 \delta a}} \quad (23)$$

and

$$E_{sp} = E^0 \pm iV \sqrt{\frac{\alpha_1}{\delta a}} \left\{ J + \frac{1}{J} + \frac{\alpha_1}{\delta a J^3} \right\} \quad (24)$$

where

$$J = \sqrt{\frac{1 \pm \sqrt{1 + 12 \left( \frac{\alpha_1}{\delta a} \right)}}{2}} \quad (25)$$

Notice that the  $V^4$  expression for the width involves factors of  $\alpha_1$  and  $\frac{V}{\delta a}$  as well as an expression that depends on the ratio  $\frac{\alpha_1}{\delta a}$ , so only by reaching the  $V^4$  level in  $E_{sp}$  and  $Z_{sp}$  is one able to access all three of  $\alpha_1$ ,  $\alpha_2$ , and  $V$  (assuming that  $\alpha_1$  is available from large- $Z$  data). We will refer to the energy and half-width of Eq. (24) as the values through order  $V^4$  in the expansion of the square root in Eq. (14).

### 3.5. Guidance for creating rational fractions

A major advantage of Padé approximants is that they provide approximations to higher order terms in the Taylor series that were not used in the fitting, and, as a result, they can often accurately represent the function at points more distant from the expansion point than can the original truncated Taylor series. However in application to stabilization calculations, one uses numerical energy data from a grid of points rather than the coefficients of a Taylor series, giving rise to what are termed RFs.

When  $Z' \gg Z_0$ , and reasonable values are chosen for the various parameters in the model, it is found that the power of  $Z$  in the numerator of the PA is essentially one higher than that in the denominator even if one constructs a PA having a higher power denominator. This is illustrated below by examining the [2,2] PA of Eq. (17) for the case  $Z' = 1.2$  and using the S3 set of ( $\alpha_1$ ,  $\alpha_2$ ,  $V$ ,  $E^0$ , and  $Z_0$ ) parameters that are defined in the next Section.

$$\text{PA}[2, 2] = \frac{1.727 - 5.069Z - 21.337Z^2}{1 - 5.334Z + 0.165 \times 10^{-4}Z^2} \quad (26)$$

Examination of this PA reveals that the coefficient of the  $Z^2$  term in the denominator is essentially 0, effectively reducing this to the [2,1] PA, which is reported along with the [1,1], and [3,2] PAs in the [Supplementary Material](#). Similarly, the [3,3] PA is found to be essentially equivalent to the [3,2] PA. For this reason only  $[n + 1, n]$  RFs are considered in the subsequent discussion. We note that the conclusion about the power of  $Z$  in the numerator being one higher than that in the denominator would be altered were one or more of  $H_{11}$ ,  $H_{22}$ , or  $V$  to assume more complicated  $Z$  dependencies than assumed here. Another observation to make is that the large- $Z$  slopes of the [2,1] and [3,2] PAs are very close to the exact value of 4.0. This shows that these low-order PAs provide accurate values for the  $a_1$  slope parameter of the model.

Using the exact energies of Eq. (14) as numerical input, we will form  $[n + 1, n]$  RFs of the form

$$\text{RF}_1 = \frac{n_0 + n_1Z + n_2Z^2}{1 + d_1Z} \quad (27)$$

and

$$\text{RF}_2 = \frac{n_0 + n_1Z + n_2Z^2 + n_3Z^3}{1 + d_1Z + d_2Z^2} \quad (28)$$

for the three sets of test data whose parameters are given in [Table 1](#). The goal of this numerical experiment is to determine the choices of  $Z$ -values for which the stationary points  $Z_{sp}$  and resonance energies of  $\text{RF}_1$  and  $\text{RF}_2$  approach the  $V^2$  or  $V^4$  or exact values (of the model). Because RFs containing  $N$  parameters are designed to represent data better than Taylor series expansions containing  $N$  parameters, we do not expect  $\text{RF}_1$  results to match  $V^2$  results or  $\text{RF}_2$  to match  $V^4$ . However, because  $\text{RF}_1$  contains four parameters, as does the  $V^2$ -level expansion of Eq. (19), we expect the  $\text{RF}_1$ - and  $V^2$ -level results to be similar. Likewise, because  $\text{RF}_2$  contains six parameters while the  $V^4$ -level expansion of Eq. (19) and the exact expression of Eq. (14) contain only five parameters, we expect  $\text{RF}_2$  to be able to match or exceed the  $V^4$ -level results.

#### 4. Comparing results of RF fits of model data to the exact, $V^2$ , and $V^4$ results

We created three sets of test data (labeled S1-S3) by inserting three choices of parameters ( $E^0$ ,  $Z_0$ ,  $a_1$ ,  $a_2$ , and  $V$ ) into Eq. (14). In all cases,  $E^0$  was taken to be 2.50 eV and  $Z_0$  was set equal to 0.200. The energy ranges and coupling strengths  $V$  are typical of low-energy electronic shape resonances in atoms and molecules. In [Table 1](#), we list the  $V$ ,  $a_1$ , and  $a_2$  parameters for each case and give where  $\delta Z$  equals  $\frac{V}{\delta a} \left( \frac{V}{\varepsilon} \right)^{\frac{1}{3}}$  or  $\frac{V}{\delta a} \left( \frac{V}{\varepsilon} \right)$  with the energy-precision parameter  $\varepsilon$  set equal to  $10^{-5}$  eV.

The  $Z$ -values shown in the third column are the  $Z$ -value bounds beyond which the  $V^4$  contribution to the energy falls below  $\varepsilon$ . Those shown in the fourth column are the bounds beyond which the  $V^2$  contribution is below this same  $\varepsilon$ .

[Fig. 2](#) depicts the exact solutions of Eq. (14) for the S1 parameter set together with two sets of data points considered in the [Supplemental Information](#). One set satisfies the  $V^4$  bound and the other does not. The figure also depicts the curves obtained from the  $\text{RF}_1$  and  $\text{RF}_2$  fits,

**Table 1**

Description of the S1, S2 and S3 parameter sets and the upper limits for  $Z$  at the  $V^4$  and  $V^2$  levels for the model given by Eq. (14).

Test Case	$V$ (eV); $a_1$ ; $a_2$	$\frac{V}{\delta a} \left( \frac{V}{\varepsilon} \right)^{\frac{1}{3}} + Z_0$ $\varepsilon = 10^{-5}$ eV	$\frac{V}{\delta a} \left( \frac{V}{\varepsilon} \right) + Z_0$ $\varepsilon = 10^{-5}$ eV
S1	0.1; 1; 10	0.439	111
S2	1.0; 1; 10	5.36	11,100
S3	0.1; 4; 6	1.28	500

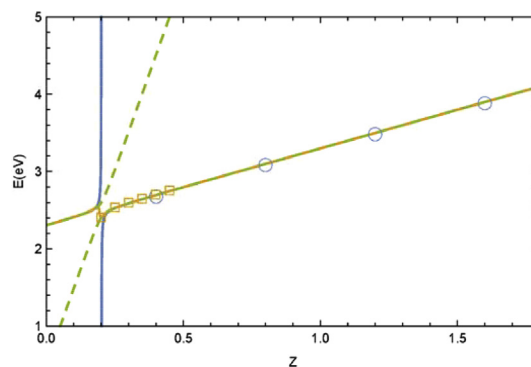


**Fig. 2.** Resonance model (Eq. (14) with the S1 parameter set. The dashed green curves represent the exact energies. The circles denote the data points listed in [Table S1-1](#), and the blue curves the  $\text{RF}_1$  fit to those points. The squares denote the data points listed in [Table S1-3](#) and the orange curves are the  $\text{RF}_2$  fits to these points.

respectively.

For any value of  $\varepsilon$ , the range of acceptable  $Z$ -values is much broader if one only wants to assure that the  $V^2$  contribution exceeds  $\varepsilon$ . The very large values listed in the right column of [Table 1](#) would likely never be realized in an ab initio stabilization plot since other avoided crossings would constrain  $Z$  to smaller values. For example, in [Fig. 1](#), the blue plateau region with energy near 0.45 eV exists only for  $Z$ -values between ca. 1 and 2 with the avoided crossing near  $Z = 2$  providing the upper limit to  $Z$ . On the other hand, the data in the third column in [Table 1](#) suggest that one has to be careful in selecting  $Z$ -values if results accurate to  $V^4$  are required to characterize the resonance.

Let us now examine for these three data sets the performance of  $\text{RF}_1$  and  $\text{RF}_2$  using various choices for  $Z$ -values at which the energies are computed. For comparison, we list in [Table 2](#) the half-widths obtained using (i) Eqs. (22) and (24) that result from expansions of the square root factor through orders  $V^2$  and  $V^4$ , respectively, and the exact values from Eq. (16).

The primary differences among cases S1-S3 are as follows:

1. S1 produces a narrow resonance ( $\Gamma/2 = 0.07$  eV) because it has both a small value for  $V$  and a large difference between  $a_1$  and  $a_2$ ;
2. S2 produces a broad resonance ( $\Gamma/2 = 0.70$  eV) because it has a large value for  $V$  (it has the same values for  $a_1$  and  $a_2$  as in S1);
3. S3 produces a broad resonance (0.49 eV) not because it has a large value for  $V$  (it has the same value as in S1) but because its slopes  $a_1$  and  $a_2$  do not differ much.

Because case S3 displays the largest differences among the  $V^2$ ,  $V^4$ , and exact half-widths, it offers the best opportunity to highlight the interplay between the energy precision ( $\varepsilon$ ) and the values of  $Z$  used to form the RF fit. For this reason, we will discuss case S3 in detail while placing analogous data for cases S1 and S2 in the [Supplementary Material](#).

##### 4.1. Results of $[n + 1, n]$ RF fits for S3

We now determine the extent to which the stationary points and

**Table 2**

Resonance half-widths (eV) sets for the model given by Eq. (14) using the S1-S3 parameter sets defined in [Table 1](#).

Test Case	$V^2$ Half-width	$V^4$ Half-width	Exact Half-width
S1	0.0667	0.0697	0.0703
S2	0.6667	0.6973	0.7027
S3	0.2828	0.3810	0.4899

**Table 3**

$Z_{sp}$  and  $E_{sp}$  (eV) from RF<sub>1</sub> fits to energy values at  $Z = 0.4, 0.8, 1.2,$  and  $1.6$  for the model described by Eq. (14) with the S3 parameter set as a function of the energy precision  $\varepsilon$  (eV).

$\varepsilon$	$Z_{sp}$	$E_{sp}$
$10^{-5}$	0.175840862 – 0.0367804471 i	2.40399052 – 0.294207598 i
$10^{-7}$	0.177067499 – 0.0366038349 i	2.40877481 – 0.292804475 i
$10^{-12}$	0.17700637 – 0.036613091 i	2.40853738 – 0.292877948 i

resonance energies obtained by fitting numerical data from Eq. (14) to RF<sub>1</sub> do or do not reproduce the results of  $V^2$  and the extent to which fitting numerical data to RF<sub>2</sub> can yield stationary points and resonance energies close to those of  $V^4$ . In Table 3 we show the results of forming an RF<sub>1</sub> using the four  $Z$ -values listed. From inspection of the stabilization plot (not shown), it was clear that  $Z = 1.6$  is well within the near-linear region while  $Z = 0.4$  is in a region of significant curvature. The real and imaginary parts of the stationary point  $Z_{sp}$ , and the real and imaginary values of the resonance energy  $E_{sp}$  are indicated for three different choices of the precision ( $10^{-5}$ ,  $10^{-7}$ , and  $10^{-12}$  eV) in the input data. In specifying the precision, we are indicating the number of figures retained to the right of the decimal point. Although in ab initio calculations the precision is likely to be limited to at most  $10^{-5}$  eV, for our model we also report results for precisions of  $10^{-7}$  and  $10^{-12}$  eV to illustrate how the results would evolve if one had more precise data.

From Table 1 it is seen that the  $V^2$  and  $V^4$  bounds for this case occur at  $Z = 500$  and  $1.28$  (for  $\varepsilon = 10^{-5}$  eV). Because all four of the  $Z$ -values employed lie well within the  $V^2$  bound, it is no surprise that the half-widths obtained at the three precision levels considered are very close to the  $V^2$  value  $0.2828$  eV listed in Table 2. Although the [2,1] RF<sub>1</sub> fit does not yield an accurate value for the half-width, it does provide an accurate  $a_1$  (4.0 as we pointed out earlier) and reasonably accurate values for  $Z_0$  (0.18 compared to the exact 0.20) and  $E^0$  (2.4 eV compared to the exact 2.5 eV).

In Table 4 we show the results of forming RF<sub>2</sub> (i.e., [3,2]) fits for the S3 parameter set using six  $Z$ -values ranging from 0.4 to 1.4; again, the smaller  $Z$ -values lie in the curved region of the stabilization plot while the larger  $Z$ -values lie in the near-linear portion of the stabilization plot.

Earlier we noted that the  $V^4$  bound for a precision of  $10^{-5}$  eV is 1.28. We see that even though five of the six  $Z$ -values used in forming this RF<sub>2</sub> fit are below 1.28, the half-width obtained using data points at the  $10^{-5}$  precision level is essentially the same as the RF<sub>1</sub> ( $V^2$ ) value. Even using [4,3], [5,4], or [6,5] RF fits with the above five  $Z$ -values below 1.28 together with additional  $Z$ -values above 1.28, at a precision of  $10^{-5}$  eV, the same  $V^2$  level half-width was obtained. This shows that it is not the level of the RF but the values of  $Z$  that prevent RF<sub>2</sub> from doing better than  $V^2$  level with data at a precision of  $10^{-5}$  eV. It also shows that one needs to have all six of the  $Z$ -values below or very near to the  $V^4$  bound because when the precision is increased to  $10^{-7}$  eV (where the  $V^4$  bound is  $Z = 5.20$ ), a half-width significantly better than the  $V^4$  value (0.38 eV) and close to the exact value (0.49 eV) is achieved.

The inability of [3,2] (or higher) fits to achieve half-widths close to (or better than as one might expect for RF fits) the  $V^4$  value with only five of six  $Z$ -values below the  $V^4$  bound and using data at  $10^{-5}$  precision

**Table 4**

$Z_{sp}$  and  $E_{sp}$  (eV) from RF<sub>2</sub> fits to energy values at  $Z = 0.4, 0.6, 0.8, 1.0, 1.2,$  and  $1.4$  for the model described by Eq. (14) with the S3 parameter set as a function of the energy precision  $\varepsilon$  (eV).

$\varepsilon$	$Z_{sp}$	$E_{sp}$
$10^{-5}$	0.185646153 – 0.0358910308 i	2.44266485 – 0.28711605 i
$10^{-7}$	0.185462414 – 0.0779571285 i	2.45378066 – 0.430534863 i
$10^{-12}$	0.188780918 – 0.076937987 i	2.46415775 – 0.426152109 i

raises the issue that we address in the next Section — namely, how to improve on the choice of  $Z$ -values by using results from the RF fits to estimate the  $V^2$  and  $V^4$  bounds and to use these results to form more accurate fits.

#### 4.2. How to improve the choice of $Z$ -values to create better $[n + 1, n]$ RF <sub>$n$</sub> fits

As noted earlier, not all of the  $Z$ -values used to form the [3,2] and higher RF fits whose results are shown in Table 4 are below the  $V^4$  bound for an energy precisions of  $\varepsilon = 10^{-5}$  eV. Moreover, any  $[n + 1, n]$  fit we tried using five  $Z$ -values below the  $V^4$  bound did not improve the situation. This suggests that we need to focus on placing at least six data points at or below the  $V^4$  bound. In the case of the S3 example, we know ahead of time where this bound is because we know the values of  $V$  and  $\delta a$ , and, as we showed earlier, these two quantities cannot be obtained from the results of the [2,1] fit. Because the [3,2] fit shown above did not improve on the [2,1] level half-width at a precision of  $10^{-5}$  eV, we cannot use the results of this [3,2] fit to obtain these parameters. However, there are two routes through which an estimate of the  $V^4$  bound can be made as we now demonstrate.

We know that a [2,1] (i.e., RF<sub>1</sub>) fit using four  $Z$ -values within the wide range below the  $V^2$  bound should be capable of yielding reasonable values for  $a_1$ ,  $Z_0$ ,  $E^0$ , and  $V^2/\delta a$ . The value of  $a_1$  is easily obtained from the slope at large  $Z$ , which for the [2,1] RF is 4.0. Knowing  $a_1$ ,  $V^2/\delta a$  can be obtained from the  $V^2$  expression for the half-width  $2\sqrt{\frac{V^2 a_1}{\delta a}}$ . Using the [2,1] results shown in Table 3 (at any of the levels of precision as they are all essentially the same), we can offer the following estimates:  $Z_0 = 0.18$ ,  $E^0 = 2.4$  eV, and  $4a_1 V^2/\delta a = (0.29 \text{ eV})^2$ , hence  $V^2/\delta a = 5.3 \times 10^{-3}$  eV. However, we need one more piece of information ( $a_2$ ) to estimate the  $V^4$  and  $V^2$  bounds.

If one has sufficient knowledge about the slope of the other diabatic state's energy far from  $Z_0$ , one can use that value as  $a_2$  and the [2,1] value of  $\frac{V^2}{\delta a}$  plus  $a_1$  obtained from the large- $Z$  slope to estimate the  $V^4$  bound as  $\delta Z = \frac{V}{\delta a} \left(\frac{V}{\varepsilon}\right)^{\frac{1}{2}}$ . This route is the most straightforward and should be followed if a reasonable estimate of  $a_2$  is available. However, in the absence of direct knowledge of  $a_2$ , another route must be found.

The fact that the [3,2] RF described in Table 4 as well as results from [4,3] and higher RFs using the  $Z$ -values in Table 5 and higher  $Z$ -values did not improve the results suggests that one or more of the  $Z$ -values used are above the  $V^4$  bound. We therefore replaced the six  $Z$ -values whose [3,2] results are shown in Table 4 by six new values ranging from  $Z = 0.25$ – $1.00$ . Doing so produced a new [3,2] RF<sub>2</sub> fit the results of which are shown in Table 5.

The first thing to notice is that the half-width obtained at a precision of  $10^{-5}$  eV has moved from 0.29 eV (see Table 4) to 0.49 eV, close to the exact value. Even when we reduced the precision to  $10^{-3}$  or  $10^{-4}$  eV, the half-width changed significantly from the  $V^2$  value of 0.29 eV. The good agreement between the width calculated using data at the  $10^{-5}$  precision level and the exact value for the width is partially fortuitous, as seen by the sizable error in the location of the stationary point and in the calculated position of the resonance. Indeed, as shown in Table 5, the half-width drops down to about 0.44 when calculated

**Table 5**

$Z_{sp}$  and  $E_{sp}$  (eV) from RF<sub>2</sub> fits to energy values at  $Z = 0.25, 0.40, 0.55, 0.70, 0.85,$  and  $1.00$  for the model described by Eq. (14) with the S3 parameter set as a function of the energy precision  $\varepsilon$  (eV).

$\varepsilon$	$Z_{sp}$	$E_{sp}$
$10^{-3}$	0.123918560 – 0.0481745490 i	2.20867287 – 0.384156255 i
$10^{-4}$	0.147948561 – 0.0406098407 i	2.29477962 – 0.324741394 i
$10^{-5}$	0.128442525 – 0.0851233013 i	2.27808877 – 0.489209000 i
$10^{-7}$	0.177648487 – 0.0797605779 i	2.42936543 – 0.439177037 i
$10^{-10}$	0.177045193 – 0.0803243612 i	2.42773751 – 0.441438257 i

using [3,2] fits at higher precision values. This indicates that for the S3 model one needs to accurately characterize contributions higher than  $V^4$  to the energy in order to accurately characterize the resonance. Indeed [4,3] and [5,4] RF fits using appropriately placed  $Z$ -values and sufficiently high precision gave half-widths near the exact value of 0.49 eV.

Seeing that placing six  $Z$ -values sufficiently low causes the new [3,2] RF to produce a half-width significantly different from that of the [2,1] RF, we now use the ratio of the new [3,2] and [2,1] half-widths to estimate the  $V^2$  and  $V^4$  bounds and to then verify whether at least six data points fall below or near to the  $V^4$  bound. To do so, we note that the exact half-width of the model is  $2\sqrt{\frac{V^2 a_1 a_2}{\delta a^2}}$ , so the ratio of the exact half-width to the [2,1] value should be  $\sqrt{\frac{a_2}{\delta a}}$ . Taking the [3,2] half-width of 0.44–0.49 eV obtained using the new set of data points as an estimate to the exact value and using 0.29 eV as the [2,1] half-width gives  $\frac{a_2}{\delta a} = 2.3$ – $2.9$ , which allows us to solve for  $a_2 = 6.1$ – $6.9$ , so we estimate  $\delta a = 2.1$ – $2.9$ . Finally, using  $V^2/\delta a = 5.3 \times 10^{-3}$ , we obtain  $V = 0.11$ – $0.12$  eV.

We can now make use of these approximations to  $a_1$ ,  $a_2$ , and  $V$ , to estimate the  $V^2$  and  $V^4$  bounds, which can then be used to improve upon the choice of  $Z$ -values used to verify the validity of the new [3,2] or to create higher RF fits. For example, assuming that we have energy data whose variation is precise to  $\varepsilon = 10^{-5}$  eV, we estimate these bounds to be (using the average of the parameter estimates given above, i.e.,  $V = 0.115$  eV and  $\delta a = 2.5$ ), we obtain  $\delta Z = \frac{V^2}{\varepsilon \delta a} = 529$  (the exact value is 500), and  $\delta Z = \frac{V}{\delta a} \left(\frac{V}{\varepsilon}\right)^{\frac{1}{3}} = 1.04$  (the exact value is 1.28). This suggests that the  $Z$ -values used to form the new [3,2] fit do lie below the  $V^4$  bound. As commented on earlier, the  $V^2$  bound is likely irrelevant in real stabilization calculations as additional avoided crossings will limit the scaling parameter; however, this path does offer a route for estimating the more important  $V^4$  bound.

This process allows us to be confident that the final six lowest  $Z$ -values in Table 5 used to form the [3,2] and higher RF fits were located in a manner that allowed us to obtain  $V^4$  quality (or higher) resonance energies and widths. It used information from the [2,1], [3,2], and higher fits obtained using  $Z$ -values some of which were above the  $V^4$  bound to guide us toward using lower  $Z$ -values for an improved [3,2] fit. This resulted in a new [3,2] fit of sufficient accuracy to generate an estimated  $V^4$  bound to offer valuable guidance about where to choose  $Z$ -values for forming a subsequent series of higher order RF fits.

In the [Supplementary Material](#) we present analogous discussions of how to find appropriate  $Z$ -values for forming [2,1] and [3,2] RFs for the S1 and S2 cases. As the reader will see, in the S2 case it became clear that one should not locate all of the  $Z$ -values too far below the  $V^4$  bound for either the [3,2] or the [2,1] RF because doing so can cause the evaluation of the  $a_1$  slope parameter to fail; one needs at least one data point in the nearly-linear region of the stabilization plot.

## 5. Conclusions and suggestions for application to ab initio stabilization plot data

A five-parameter model of a stabilization graph which is based on two diabatic states undergoing an avoided crossing, is used to generate test data (energy vs. a scaling parameter  $Z$ ) for creating RF approximants. Our analysis allowed us to conclude that:

1. when forming a  $RF_1$  approximant to achieve results accurate to order  $V^2$ , one needs to use four (or more, if least squares fitting to determine parameters) data points below  $Z = Z_0 + \frac{V}{\delta a} \frac{V}{\varepsilon}$  where the second order contribution to the energy falls below the precision  $\varepsilon$  to which the energies are known ( $\varepsilon$  of ca.  $10^{-5}$  eV range was assumed), but it is also important to include at least one point in the quasi-linear portion of the stabilization plot to extract the  $a_1$  slope parameter;

2. when forming a  $RF_2$  approximant to achieve results accurate to order  $V^4$ , one needs to use six (or more, if least squares fitting to determine parameters) data points below or very near  $Z_0 + \frac{V}{\delta a} \left(\frac{V}{\varepsilon}\right)^{\frac{1}{3}}$  beyond which the fourth order contributions fall below  $\varepsilon$ , but again it is important to include at least one point in the quasi-linear region to extract  $a_1$ .

We also note that stabilization graphs for real molecular resonances often require fits with eight or more parameters to extract an accurate value of the resonance width [15]. This indicates the importance of higher-order  $V$ -dependence than  $V^4$ , which would force one to select data points even closer  $Z_0$  than  $Z_0 + \frac{V}{\delta a} \left(\frac{V}{\varepsilon}\right)^{\frac{1}{3}}$ . For example, if terms of the order  $V^6$  were important, one would have to choose points at or below  $Z_0 + \frac{V}{\delta a} \left(\frac{2V}{\varepsilon}\right)^{\frac{1}{3}}$ , which would be  $Z = 0.28, 1.48,$  and  $0.56$  for S1, S2, and S3, respectively. In our opinion, these facts argue in favor of using the QE-type methods rather than RFs that emphasize the quasi-linear large- $Z$  regions of stabilization graphs.

Based on these observations, we suggest a strategy to use in constructing a  $[n + 1, n]$  RF representation of data on a single branch of a stabilization plot involving ab initio data in a manner that begins with first identifying a quasi-linear plateau region. For such cases, one generally does not know ahead of time how to select points optimal for accurately determining the metastable state's energy and width because one does not know how close to the more curved region of the stabilization plot one must characterize to achieve results of reasonable accuracy. However, the results obtained here can provide guidance if the ab initio stabilization plot displays two essential features that our model relies upon- (i) a portion that varies approximately linearly with  $Z$  at large- $Z$  (described in our model by the terms  $E^0 + a_1(Z - Z_0)$ ) and (ii) a part (arising in our model from the term  $\pm \sqrt{V^2 + \left[\frac{\delta a}{2}(Z - Z_0)\right]^2}$ ) with curvature that increases in magnitude as  $Z$  moves closer to the avoided-crossing point  $Z_0$ .

For a stabilization plot that shows these characteristics, we suggest the following pathway can allow one to confidently evaluate the reliability of a RF and of the location of its data points.

- i. First, one should search the energy data set for a region sufficiently far from  $Z_0$  for which the energy varies approximately linearly with  $Z$ . The slope in this region can be associated with  $a_1$  of our model. We suggest looking at our discussion of the S2 case in the [Supplementary Material](#) where our first choice of  $Z$ -values did not meet this criterion, and consequently, reasonable values of the resonance parameters did not result.
- ii. Then, one should examine the data set at smaller  $Z$ -values until finding a region where the data begin to deviate significantly from the near-linear form found in step i. Using at least one data point in the near-linear region and the remaining data points in the region of significant curvature, one can form a  $RF_1$  approximant.
- iii. Since the stationary points of  $RF_1$  are expected to occur near the  $V^2$  value of  $Z_{sp} = Z_0 \pm \frac{iV}{\sqrt{a_1 \delta a}}$  where the complex energy is  $E_{sp} = E^0 \pm 2iV \sqrt{\frac{a_1}{\delta a}}$ , one can use  $Z_{sp}$  and  $E_{sp}$  to estimate three more model-system parameters (with  $a_1$  having been estimated from the near-linear region's slope)

$$\frac{V^2}{\delta a} = a_1 (\text{Im}(Z_{sp}))^2; \quad (29)$$

$$E^0 = \text{Re}(E_{sp}); \quad (30)$$

and

$$Z_0 = \text{Re}(Z_{sp}) \quad (31)$$

This knowledge then allows one to compute  $Z = Z_0 + \frac{V}{\delta a} \frac{V}{\varepsilon}$ , which

one can use to verify whether the four data points used to create the ab initio RF<sub>1</sub> lie below the  $V^2$  bound. If not, it is recommended that one adjust the choice of  $Z$ -values to form a new RF<sub>1</sub>. However, as noted earlier, it is likely that all  $Z$ -values between successive avoided crossings lie within this  $V^2$  bound in ab initio stabilization graphs.

- iv. If one has a reasonable estimate of  $a_2$ , one can multiply the  $V^2$  width by the ratio  $\sqrt{\frac{a_2}{a_2 - a_1}}$  (see Eq. (16)) to obtain an estimate of the exact width. Moreover, knowing  $a_2$ , one has enough knowledge to evaluate the point  $Z_0 + \frac{V}{\delta a} \left(\frac{V}{\varepsilon}\right)^{\frac{1}{3}}$  at which the  $V^4$  contributions to the energy fall below  $\varepsilon$ , so one can estimate where to place data points in forming a subsequent RF<sub>2</sub> approximant.
- v. If one does not have a good estimate for  $a_2$ , to form RF<sub>2</sub>, one can search the energy data for a range even closer to the crossing point within which the energy deviates significantly from  $E^0 + a_1(Z - Z_0) - \frac{V^2}{\delta a(Z - Z_0)}$  (using the values of  $E^0$ ,  $a_1$ ,  $Z_0$  and  $\frac{V^2}{\delta a}$  obtained in step iii). One can then use at least six data points in the region where the data deviates from  $E^0 + a_1(Z - Z_0) - \frac{V^2}{\delta a(Z - Z_0)}$  (being careful to include one point as near as possible to the near-linear region) to form a RF<sub>2</sub> approximant. As outlined earlier, the ratio of the half-width obtained from the RF<sub>2</sub> to that from the RF<sub>1</sub>, is approximately  $\sqrt{\frac{a_2}{\delta a}}$ , which allows one to estimate  $a_2$ .

Knowing all five parameters of a model derived from the ab initio RF<sub>1</sub> and RF<sub>2</sub> then allows one to compute the point at which the fourth order contributions to the energy fall below  $\varepsilon$ :  $Z_0 + \frac{V}{\delta a} \left(\frac{V}{\varepsilon}\right)^{\frac{1}{3}}$  and to thus verify whether all of the  $Z$ -values used to form the RF<sub>2</sub> approximant in step v lie below  $Z_0 + \frac{V}{\delta a} \left(\frac{V}{\varepsilon}\right)^{\frac{1}{3}}$ . Knowing even approximate values for  $\frac{V}{\delta a}$  and (especially)  $\frac{V}{\delta a} \left(\frac{V}{\varepsilon}\right)^{\frac{1}{3}}$  would allow one to wisely choose  $Z_k$  values in forming any higher-order  $[n + 1, n]$  RF approximant of the ab initio data, and it is likely that such higher-order RFs would then produce the most reliable  $E_{sp}$  and  $Z_{sp}$  values to use in ab initio determinations of resonance-state energies and lifetimes.

## Acknowledgments

KG acknowledges the support of a graduate fellowship from the

Pittsburgh Quantum Institute. This research was supported by grant number CHE1762337 from the U.S. National Science Foundation. We also acknowledge the use of computational resources in the University of Pittsburgh's Center for Research Computing.

## Appendix A. Supplementary data

Supplementary data associated with this article can be found, in the online version, at <https://doi.org/10.1016/j.chemphys.2018.07.019>.

## References

- [1] A.U. Hazi, H.S. Taylor, Stabilization method of calculating resonance energies: model problem, *Phys. Rev. A* 1 (1970) 1109–1120.
- [2] J.S.-Y. Chao, M.F. Falcetta, K.D. Jordan, Application of the stabilization method to the  $N_2^-$  ( $X^2\Pi_g$ ) and  $Mg^-(1^2P)$  temporary anion states, *J. Chem. Phys.* 93 (1990) 1125–1135.
- [3] J. Horáček, I. Páidarová, R. Čurík, Determination of the resonance energy and width of the  $^3B_{2g}$  shape resonance of ethylene with the method of analytical continuation in the coupling constant, *J. Phys. Chem. A* 118 (2014) 6536–6541.
- [4] J.F. Stanton, J. Gauss, Perturbative treatment of the similarity transformed hamiltonians in equation-of-motion couple-cluster approximations, *J. Chem. Phys.* 103 (1995) 1064–1076.
- [5] M. Nooijen, R.J. Bartlett, Equation of motion couple cluster method for electron attachment, *J. Chem. Phys.* 102 (1995) 3629–3647.
- [6] T. Koopmans, On the assignment of wave functions and eigenvalues to the individual electrons of an atom, *Physica* 1 (1934) 104–113.
- [7] J. Schirmer, L.S. Cederbaum, O. Walter, New approach to the one-particle green's function for finite fermi systems, *Phys. Rev. A* 28 (1983) 1237–1259.
- [8] I. Haritan, N. Moiseyev, On the calculation of resonances by analytic continuation of eigenvalues from the stabilization graph, *J. Chem. Phys.* 147 (014101) (2017) 1–9.
- [9] A.J.F. Siegert, On the derivation of the dispersion formula for nuclear reactions, *Phys. Rev.* 56 (1939) 750–752.
- [10] C.W. McCurdy, J.F. McNutt, On the possibility of analytically continuing stabilization graphs to determine resonance positions and widths accurately, *Chem. Phys. Lett.* 94 (1983) 306–310.
- [11] G.A. Baker Jr., P. Graves-Morris, *Padé Approximants*, Cambridge Univ Press, 1996.
- [12] K.D. Jordan, Construction of potential energy curves in avoided crossing situations, *Chem. Phys.* 9 (1975) 199–204.
- [13] L. Schlessinger, Use of analyticity in the calculation of nonrelativistic scattering amplitudes, *Phys. Rev.* 167 (1968) 1411–1423.
- [14] J. Simons, Resonance lifetimes from stabilization graphs, *J. Chem. Phys.* 75 (1981) 2465–2467.
- [15] K. Gasperich, K. D. Jordan, unpublished results.